Modelling the hot electron spectrum in exothermic reactions on metals

Modelling the hot electron spectrum in exothermic reactions on metals

Massimo Tomellini

Dipartimento di Scienze e Tecnologie Chimiche Università di Roma Tor Vergata Via della Ricerca Scientifica, 00133 Roma, Italy

Abstract
A phenomenological model is developed to describe the process of energy disposal, ruled by electron–hole pair generation, in exoergic processes at metal surfaces. The evolution of the energy distribution function of the metal electrons has been studied in the case of exoergic adsorption of gas atoms. A simple expression is derived for the chemicurrent yield which applies to both adsorption and recombination phenomena. The model is employed for interpreting experimental data on hot carrier generation by H adsorption. A comparison between the results of the present theory and those previously obtained by means of other approaches is also reported and discussed.

1. Introduction

In exoergic reactions at solid surfaces the energy disposal of the reacting species is an important process since it can substantially affect the reaction mechanism. For instance, in the case of atom recombination the transition from a classical LH (Langmuir–Hinshelwood) to an HA (hot atom) [1] mechanism has been shown to be driven by the ratio between the probability for diatom formation and that for the dissipation of the adatom energy into the solid [2, 3]. At metal surfaces the chemical energy released by the reaction brings about the generation of electron–hole (e–h) pairs, as experimentally demonstrated through the measurements of the chemicurrent yield [4–6]. These measurements give information on the efficiency of the e–h excitation process. As a matter of fact, chemicurrent yields show that the energy disposal via e–h pair formation is quite efficient when H or O atoms interact with the metal surface, in the case of molecules with strong adsorption energies, (e.g. NO), and in the case of adspecies with small adsorption energies as well (e.g. CO_2) [5]. These experimental results have been described in [5] by considering a mean value of the energy transferred to the e–h pairs equal to $0.3E_a$, with E_a being the adsorption energy. In this context it is worth citing the recent work on the relaxation of vibrationally excited NO ($\nu = 15$) on Au(111) via e–h pair generation where multiple quanta of vibrational energy are transferred to a single e–h pair [7].

Analytical and numerical simulations give the probability distribution function for the energy disposal via e–h pair formation and indicate that the width of this distribution and the average value of the energy transfer per scattering event can be quite large [8, 9], in accord with the chemicurrent measurements. Theoretical models on chemicurrent yield and on the time dependence of the non-equilibrium electron distribution function have recently been presented [10–14]. In [10] the energy loss via e–h pair formation is described through a position dependent friction coefficient, for an adsorbate moving near the metal surface, that is computed by means of an *ab initio* approach. This method is applied to the H and D adsorption on Cu(111) and gives a theoretical estimate of the chemically induced current that is in agreement with the experimental results. In [11, 12] the process of energy dissipation into e–h pairs has been simulated using time dependent density functional theory for H atoms interacting with an Al(111) surface. The hot electron spectrum was also obtained and it is found to be characterized, approximately, by an exponential decay. In [13] the hot electron spectrum has been computed analytically by using the Newns–Anderson model for a spin polarized adsorbate approaching the surface. This method also allows us to investigate the validity of a friction based approach as well as a useful check of simulations based on *ab initio* time dependent density functional theory. In [14] the energy distribution of metal electrons during H-atom recombination has been computed under steady state conditions and for a continuous distribution of vibrational states of the adatoms.

In the case of energy disposal dominated by e–h pair excitation, it has been shown how the spectrum of hot electrons is governed by the energy distribution function of the adatoms in the adsorption potential well. The coupling between these two distributions has been further investigated through the principle of detailed balance [14] which provides a relationship

between the forward and the reverse rate constants for energy transfer to the electron gas (reservoir). In this context it was shown that the non-equilibrium state of the electron gas affects the energy distribution of the adatoms the larger the excitation energy of the e–h pair is.

The non-adiabatic excitation of e–h pairs and the detection of chemicurrents have been analysed in detail in [15] by means of a three-step model. The following independent steps have been considered: (i) hot electron generation at the metal surface; (ii) hot carrier transport across the metal film and (iii) energy transmission through the Schottky barrier.

The purpose of the present contribution is mainly confined to the first two processes that are described in the framework of the Boltzmann transport equation where the e–h pair excitation is taken into account by appropriate boundary conditions. As far as step (iii) is concerned, the transmission coefficient across the metal–semiconductor interface is assumed to be a unit step function for energies higher than the Schottky barrier. Also, in this contribution we extend the approach of [14] to the adsorption phenomenon in order to study the time evolution of the electron spectrum. Unlike the previous analysis [14] the electron spectrum will be studied under non-steady state conditions and in dependence on the distance from the surface. The theoretical model allows one to estimate the chemicurrent yield and leads to a formula that holds for both recombination and adsorption processes.

2. Results and discussion

As outlined in the introduction, we deal with exoergic reactions where the energy released is transferred to the solid leading to e–h pair excitation. A schematic representation of the energetics of the process is depicted in figures 1(a) and (b). Adatoms enter the adsorption well from the upper bound level and 'move down' the well owing to the exchange of the energy quantum ΔE (figure 1(c)). Figures 1(a) and (b) refer to the energetics of reactive and non-reactive adsorption, respectively. By the term reactive adsorption we mean atom adsorption followed by recombination and desorption of the diatom A_2 (figure 1(a)). Non-reactive adsorption, on the other hand, refers to the adsorption of an adspecies (B in figure 1(b)) that does not recombine on the surface (e.g. CO).

Let us first consider reactive adsorption. The adsorption energy as measured with respect to the gas species is given by $[\frac{1}{2}D_{A_2} + E_a]$ where D_{A_2} is the diatom binding energy and E_a is the adatom adsorption energy as measured with respect to the A_2 molecule at rest and vibrationless (figure 1(a)). In the low coverage regime, the rate of diatom formation is small and adsorption prevails. As the process proceeds the surface coverage increases and a steady state regime is eventually reached when the adsorption rate, J, equals the recombination rate, Φ (figure 1(a)). At steady state the energy dissipation into the metal occurs at the constant rate $\frac{1}{2}D_{A_2}\Phi$ and, consequently, a non-equilibrium stationary state of the adlayer is generally achieved [3]. In the non-reactive case, depicted in figure 1(b), the steady state regime is obtained when the adsorption reaches completion, that is when the adsorption rate, F, vanishes and the equilibrium condition is obtained.
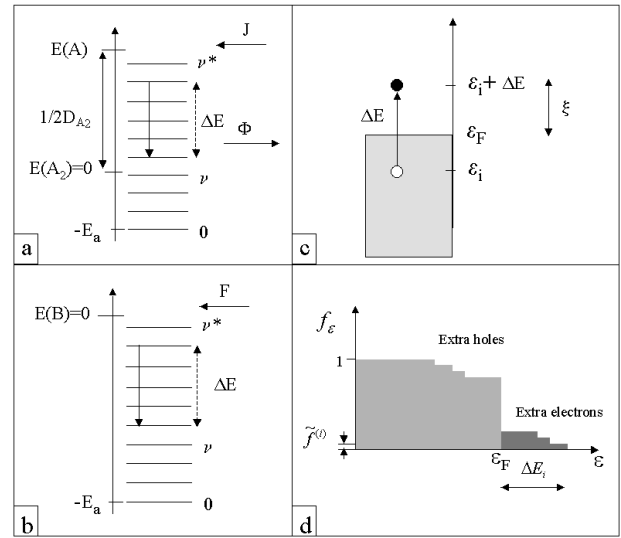
Figure 1. Schematic representation of the e–h pair excitation process via adatom relaxation in the adsorption well. The adatom vibrational ladders, in the cases of both atom recombination and adsorption, are displayed in panels (a) and (b), respectively. D_{A_2} is the binding energy of the diatom, E_a the adsorption energy, J and F are the fluxes of gas species entering the ladders and Φ is the recombination rate. A pictorial view of the e–h pair excitation process at the metal surface is also depicted in panel (c). ΔE is the energy transferred by the adatom to the electron gas, ν^* the upper bound level and ε_F the Fermi energy. A representation of the non-equilibrium electron distribution function is show in panel (d). A uniform distribution of extra electrons (holes) is assumed to arise from each dissipation channel with energy loss ΔE_i. The whole distribution is eventually obtained by summing all these contributions.

Let us now shift to the process of energy transfer to the metal electrons and to the modelling of their non-equilibrium energy distribution function. The e–h pair excitation is thought to occur in a surface layer whose thickness, δ, is negligible when compared to the mean free path of the electrons, λ [6]. The electron distribution function, f, can be determined through the Boltzmann equation together with the relaxation time *ansatz* [16]. Since f depends on both time and spatial coordinate along the internal normal to the surface plane, x, we get

$$\frac{\partial \tilde{f}_\varepsilon}{\partial t} + v_x \frac{\partial \tilde{f}_\varepsilon}{\partial x} = -\frac{\tilde{f}_\varepsilon}{\tau}. \qquad (1)$$

In equation (1) $\tilde{f}_\varepsilon = f_\varepsilon - f_\varepsilon^{(0)}$, with $f_\varepsilon^{(0)}$ being the Fermi–Dirac equilibrium distribution, v_x is the electron velocity, ε the electron energy and τ the relaxation time. This last quantity includes both electron–electron (ee) and electron–phonon (ep) relaxation channels, $\tau^{-1} = \tau_{ee}^{-1} + \tau_{ep}^{-1}$, where $\tau_{ee} < \tau_{ep}$ is expected to hold. For the sake of simplicity, in the following the relaxation time and the electron velocity are assumed to be independent of energy. We consider, first, the case in which the relaxation of the adspecies, within the adsorption well, occurs through the exchange of energy quanta of magnitude ΔE. In addition, since to a first approximation the electron and the hole distributions are symmetric in energy [14], we confine our analysis to the case $\xi = \varepsilon - \varepsilon_F > 0$, where ε_F is the Fermi energy.

The boundary condition of equation (1) is obtained by exploiting the conservation of the electron flux in the layer where the excitation takes place. Let us designate with $c_e(t)$ the concentration of hot electrons in this surface layer. One assumes that the velocity of these 'nascent' hot electrons is distributed at random within the 4π solid angle, with the same modulus of the velocity, v. In the following $v = v_F$ is assumed, with v_F being the Fermi velocity. Conservation of the number of electrons requires that the generation rate of hot electrons equals the rate at which they leave the surface layer. Denoting by $F_{ex}(t)$ the energy power (per adspecies) used in the creation of e–h pairs, with M being the surface density of adsorption sites at the bare surface, and with ΔE the excitation energy of the e–h pairs, the flux balance becomes

$$\frac{M F_{ex}(t)}{\Delta E} = \int_{\frac{\Omega_0}{2}} c_e(t) v_F \cos\vartheta \frac{d\Omega}{\Omega_0} + c_e(t)\frac{\delta}{\tau}, \quad (2)$$

where $\cos\vartheta$ is the component of the velocity versor along the internal normal to the surface, $\Omega_0 = 4\pi$ and the integration is performed over the $\frac{\Omega_0}{2} = 2\pi$ solid angle. The last term in equation (2) accounts for the *ee* and *ep* scatterings leading to the thermalization of hot carriers. From equation (2) one eventually gets

$$\frac{M F_{ex}(t)}{\Delta E} = c_e(t) v_F \left(\frac{1}{4} + \frac{\delta}{\lambda}\right) \cong c_e(t)v, \quad (3)$$

where $v = v_F/4$ and the approximation $\delta/\lambda \ll 1$ was employed. Furthermore, the energy distribution function of the excited electrons in the surface layer ($x = 0$) can be linked to equation (3) as follows:

$$c_e(t) = \rho \int_0^\infty \tilde{f}_{\xi, \Delta E}(0, t)\, d\xi = \frac{M F_{ex}(t)}{v \Delta E} \quad (4)$$

where $\xi = \varepsilon - \varepsilon_F$ and ρ is the electron density of states, which is considered to be constant. Equation (4) assumes, at any given time, a uniform distribution of *hot* electrons for $\xi \leqslant \Delta E$ (figure 1(d)) and a quasi steady state condition. This last requirement is expected to be fulfilled since the timescale over which $F_{ex}(t)$ changes is much longer than the residence time of the hot electrons in the layer. A representation of the non-equilibrium electron distribution function is shown in figure 1(d) for the general case of several relaxation routes with energy loss ΔE_i. From equations (3) and (4) the boundary condition is then obtained according to

$$\tilde{f}_{\xi, \Delta E}(0, t) = \frac{M F_{ex}(t)}{\rho v \Delta E^2}\Theta(\Delta E - \xi), \quad (5)$$

where $\Theta(x)$ is the Heaviside function and $F_{ex}(t)$ is linked to the adsorption kinetics. By performing the Laplace transform of $\tilde{f}_{\xi, \Delta E}(x, t)$ equation (1) becomes

$$\frac{\partial \varphi_{\xi, \Delta E}(x, s)}{\partial x} = -\frac{\alpha(s)}{v_x}\varphi_{\xi, \Delta E}(x, s), \quad (6)$$

where $\alpha(s) = (s + \tau^{-1})$ and the initial condition $\tilde{f}_\xi(x, 0) = 0$ has been assumed. By setting $v_x \cong v$ the solution of equation (6) is

$$\varphi_{\xi, \Delta E}(x, s) = \varphi_{\xi, \Delta E}(0, s)e^{-\alpha(s)x/v}, \quad (7)$$

with $\varphi_{\xi, \Delta E}(0, s)$ being the Laplace transform of equation (5).

The $F_{ex}(t)$ function is computed by modelling the adsorption kinetics in the framework of a 'hit and stick' process

$$\dot{\sigma} = \frac{1}{\tau_a}e^{-t/\tau_a}, \quad (8)$$

where $\dot{\sigma}$ is the adsorption rate and τ_a the characteristic time for adsorption. It is important to remember that the adatom energy can be channelled into dissipation routes other than e–h pair excitation. Collective excitations, such as phonons, can take place during adsorption as well. This can be considered in the computation of $F_{ex}(t)$ by introducing the probabilities p_{eh} and p_{ph} with $p_{eh} + p_{ph} = 1$, which are, respectively those for energy relaxation occurring via e–h or phonon excitation. Then, $F_{ex}(t) = \dot{\sigma} p_{eh} E_a = \frac{p_{eh} E_a}{\tau_a}e^{-t/\tau_a}$ where E_a is the adsorption energy and p_{eh} is taken as constant. It follows that

$$\varphi_{\xi, \Delta E}(0, s) = \frac{M p_{eh} E_a}{\rho v \Delta E^2}\frac{1}{\tau_a}\frac{1}{(s + \tau_a^{-1})}\Theta(\Delta E - \xi), \quad (9)$$

which eventually leads to the solution

$$\tilde{f}_{\xi, \Delta E}(\bar{x}, \bar{t}) = \frac{M p_{eh} E_a \gamma}{\rho \lambda \Delta E^2}e^{-\bar{x}}e^{-(\bar{t} - \bar{x})\gamma}\Theta(\bar{t} - \bar{x})\Theta(\Delta E - \xi), \quad (10)$$
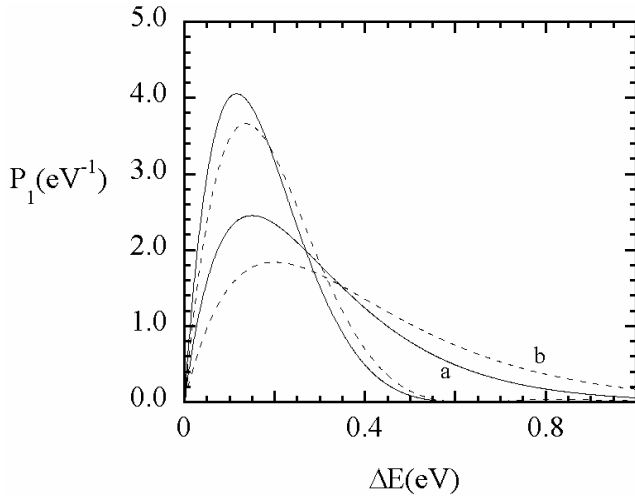
where λ is the electron mean free path and the non-dimensional quantities $\bar{t} = t/\tau$, $\bar{x} = x/v\tau \cong x/\lambda$ and $\gamma = \tau/\tau_a$ have been defined.

In order to deal with the excitation of e–h pairs of different energy, equation (10) has to be summed over ΔE by assigning a weight factor to each term of the sum (figure 1(d)). This can be done by using the results of [8] and exploiting the continuum limit. The probability that the adatom loses an energy $\Delta E = \hbar\omega$ in a single reaction event (in a round trip) has been computed in [8] by employing a strong-coupling boson description in the case of perturbations that vary slowly in time. In this model the nuclear motion of the adatom is treated classically and the particle trajectory is calculated under the assumption that no energy is lost. As discussed in [8], this inconsistency should not be important for the non-adiabatic effects that usually occur when the particle velocity is much larger than its initial velocity. The expression of the e–h pair excitation probability is formally similar to that obtained for the forced oscillator model [8]: $P(\omega) = \frac{1}{2\pi}\int_{-\infty}^{+\infty} dt e^{i\omega t} P_0 \exp[\sum_i \frac{|\lambda_i|^2}{(\hbar\omega_i)^2}e^{-i\omega_i t}]$ where $P_0 = \exp[-\sum_i \frac{|\lambda_i|^2}{(\hbar\omega_i)^2}]$, $\hbar\omega_i$ is the energy of the e–h pair and $\lambda_i \equiv \lambda(\omega_i)$ is the Fourier transform of the time derivative of the interaction potential. By means of this expression it is possible to evaluate the probability distribution function for the single e–h excitation, $P_1(\omega)$. In fact, by Taylor expanding the exponential term in the $P(\omega)$ expression one eventually gets [17]

$$P_1(\omega) = P_0 \sum_i \frac{|\lambda_i|^2}{(\hbar\omega_i)^2}\delta(\omega - \omega_i). \quad (11)$$

Once computed in the continuum limit and for a constant density of states, $D(\omega) \equiv D$, equation (11) gives

$$P_1(\omega) = \frac{1}{\hbar^2}\int_{\omega_F - \omega}^{\omega_F} P_0 \omega^{-2}|\lambda(\omega)|^2 D(\omega')D(\omega' + \omega)\, d\omega'$$
$$= P_0 \frac{D^2}{\hbar^2 \omega}|\lambda(\omega)|^2, \quad (12)$$

Figure 2. Probability distribution functions for the single e–h pair excitation. The distribution given by equation (13) has been shown as solid lines for $\varepsilon_0 = 0.1$ eV and $\eta = 0.15$ eV and as dashed lines for $\varepsilon_0 = 0.1$ eV and $\eta = 0.2$ eV. The probability curves, as obtained by Taylor expanding the cosine function in equation (13), are also shown as a solid line ($\eta = 0.15$ eV, curve a) and a dashed line ($\eta = 0.2$ eV, curve b).

where $\omega_F = \varepsilon_F/\hbar$. $|\lambda(\omega)|^2$ has been estimated in [8] in the case of strong coupling when an adsorbate level crosses the Fermi level during its motion toward the surface. The result reads: $|\lambda(\omega)|^2 \propto [1 - \cos(\omega/\omega_0)]e^{-\omega/\omega_1}$ where ω_0^{-1} and ω_1^{-1} are of the order of magnitude of the round trip time and crossing time of the adatom, respectively [8]. In the limiting case of single pair excitation the normalized probability distribution function then becomes

$$P_1(w) = \frac{2}{\ln\left[1 + (\eta/\varepsilon_0)^2\right]} \frac{e^{-w/\eta}}{w} [1 - \cos(w/\varepsilon_0)], \quad (13)$$

where w is the energy loss, $\eta = \hbar\omega_1$ and $\varepsilon_0 = \hbar\omega_0$. The first moment of the distribution, i.e. the mean energy of the single excitation, is given by $\langle\Delta E\rangle = [1 + (\varepsilon_0/\eta)^2]^{-1} \frac{2\eta}{\ln[1+(\eta/\varepsilon_0)^2]}$. In addition, the inequality $\eta \geqslant \varepsilon_0$ is expected to hold. One observes that by expanding the cosine function in equation (13) up to the second-order term, the probability distribution function reduces to $P_1(w) \cong \frac{we^{-w/\eta}}{\eta^2}$, with $\eta = \langle\Delta E\rangle/2$. However, with the aim of describing the chemicurrent yield, the condition $w < \eta$ cannot be employed since the height of the Schottky barrier is usually larger than the mean value of the energy loss. Typical behaviours of the probability distribution curve, together with its approximate expression derived above, are shown in figure 2.

By integrating equation (10) over the probability distribution function, equation (13), the electron spectrum is eventually obtained as

$$\tilde{f}_\xi(\bar{x}, \bar{t}) = \frac{M E_a \gamma p_{eh}}{\rho\lambda} \frac{\Gamma_{\eta/\varepsilon_0}}{\varepsilon_0^2} e^{-\bar{x}} e^{-(\bar{t}-\bar{x})\gamma} \psi_{\xi/\varepsilon_0} \Theta(\bar{t} - \bar{x}), \quad (14)$$

where $\Gamma_{\eta/\varepsilon_0} = \frac{2}{\ln[1+(\eta/\varepsilon_0)^2]}$ and $\psi_{\xi/\varepsilon_0} \cong \int_{\xi/\varepsilon_0}^{\infty} \frac{e^{-z\varepsilon_0/\eta}(1-\cos z)}{z^3} dz$. For $E_a/\eta > 1$, to a first approximation the upper integration limit of this integral is taken as infinite.
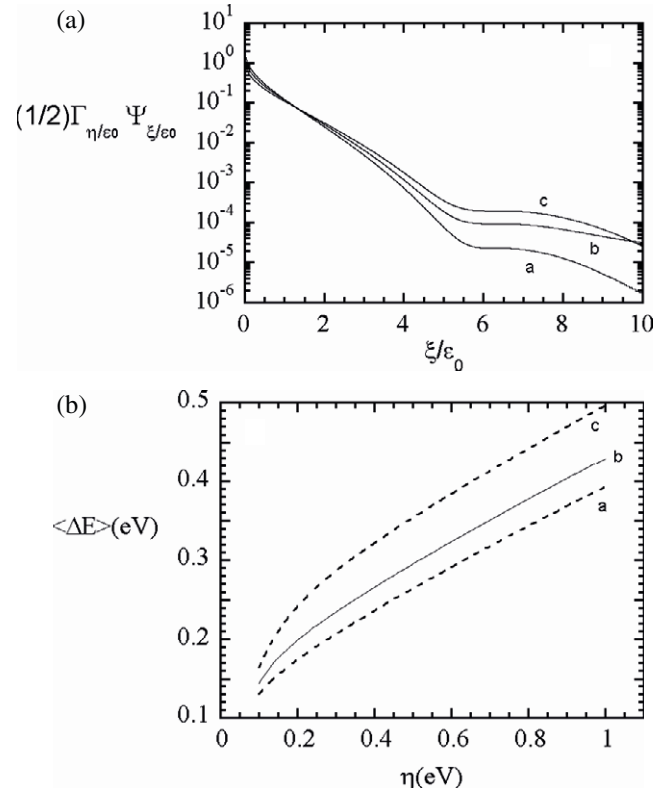
Figure 3. Behaviour of the energy distribution function of the surface electrons during chemisorption on metals. Computations are for the time domain that is characteristic of the adsorption process (equation (15b)). Panel (a) shows the function $\frac{1}{2}\Gamma_{\eta/\varepsilon_0}\psi_{\xi/\varepsilon_0}$ computed for $\varepsilon_0 = 0.1$ eV and $\eta = 0.15$ eV (curve a), $\eta = 0.2$ eV (curve b) and $\eta = 0.3$ eV(curve c). In panel (b) the dependence of the average value of the energy loss, $\langle\Delta E\rangle$, on η is displayed for $\varepsilon_0 = 0.08$ eV (curve a), $\varepsilon_0 = 0.1$ eV (curve b) and $\varepsilon_0 = 0.14$ eV (curve c).

By noting that τ is several orders of magnitudes smaller than τ_a, two time domains can be singled out in equation (14): (i) $t \approx \tau \ll \tau_a$ and (ii) $t \approx \tau_a \gg \tau$. In these two cases equation (14) becomes

$$\tilde{f}_\xi(\bar{x}, \bar{t}) \cong \frac{M E_a \gamma p_{eh}}{\rho\lambda\varepsilon_0^2} \Gamma_{\eta/\varepsilon_0} e^{-\bar{x}} \psi_{\xi/\varepsilon_0} \Theta(\bar{t} - \bar{x}) \quad \text{(case i)} \quad (15a)$$

$$\tilde{f}_\xi(\bar{x}, t) \cong \frac{M E_a \gamma p_{eh}}{\rho\lambda\varepsilon_0^2} \Gamma_{\eta/\varepsilon_0} e^{-\bar{x}} e^{-t/\tau_a} \psi_{\xi/\varepsilon_0}$$

$$= \frac{M E_a \gamma p_{eh}}{\rho\lambda\varepsilon_0^2} \Gamma_{\eta/\varepsilon_0} (1 - \sigma(t)) e^{-\bar{x}} \psi_{\xi/\varepsilon_0}, \quad \text{(case ii)} \quad (15b)$$

where in equation (15b), that is in the adsorption timescale, the Heaviside function can be taken as equal to 1. It is worth noting that for the free electron gas the term $\frac{\gamma}{\rho\lambda} = (\tau_a \upsilon\rho)^{-1}$ depends upon the surface electron density, n, since both ρ and υ scale as $n^{1/3}$. To be specific $(\upsilon\rho) \cong \frac{1}{2(3\pi^2)^{1/3}\hbar}n^{2/3}$, where $\upsilon = \upsilon_F/4$ and $\rho = n/\varepsilon_F$ were used. We confine the present analysis to the time domain characteristic of the adsorption kinetics. The behaviour of the normalized energy distribution function of the electrons, $\frac{1}{2}\Gamma_{\eta/\varepsilon_0}\psi_{\xi/\varepsilon_0}$, is displayed in figure 3(a) for several values of η and at $\varepsilon_0 = 0.1$ eV. In fact, this ε_0 figure has been chosen in accord with the typical values of the round trip time of the adatom as obtained by means of
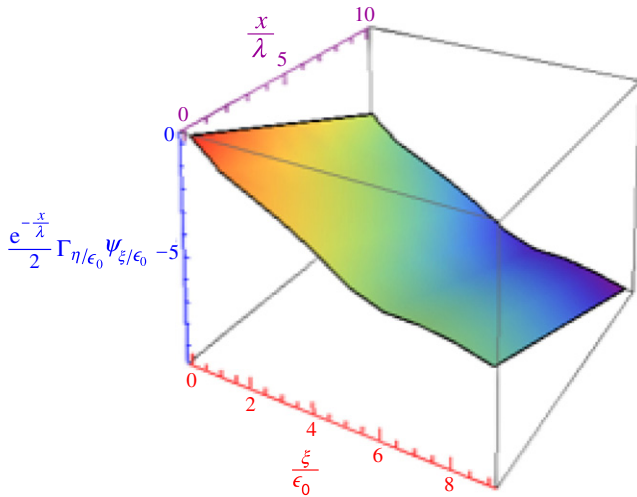
Figure 4. Three-dimensional plot of the hot electron spectrum as a function of the dimensionless variables ξ/ε_0 and x/λ. Parameter values are: $\sigma = 0$, $\varepsilon_0 = 0.1$ eV and $\eta = 0.15$ eV. The distribution function has been normalized to the pre-factor $\frac{2ME_{eh}\gamma}{\rho\lambda\varepsilon_0^2}$.

(This figure is in colour only in the electronic version)

the *ab initio* method [10, 18]. In particular, for the H/Cu system this elapsed time was estimated to be 0.04 ps, which implies $\varepsilon_0 \cong 0.1$ eV. For the typical values $M = 10^5$ cm^{-2}, $\tau_a = 20$ s, $E_a = 1$ eV, $n = 10^{22}$ cm^{-3} and $\varepsilon_0 = 0.1$ eV the term $\frac{ME_a}{\tau_a \upsilon \rho \varepsilon_0^2}$ in equation (15*b*) is about 4×10^{-14}. In figure 3(b) the mean value of the energy loss has also been shown, as a function of η, for $\varepsilon_0 = 0.14$ eV, $\varepsilon_0 = 0.1$ eV and $\varepsilon_0 = 0.08$ eV. Furthermore, a 3D plot of the electron energy distribution function has been reported in figure 4 as a function of x/λ and ξ/ε_0 at $\sigma \ll 1$. Since the approximation employed to estimate ψ_{ξ/ε_0} is better the larger the E_a/η ratio is, the results of figures 3 and 4 are to be considered more reliable the higher this ratio is. The function ψ_{ξ/ε_0} exhibits a divergence at $\xi = 0$ that is removed once the integral of the chemicurrent yield is carried out (equation (16)). Specifically, from the computation above one evaluates the number of electrons (per adsorbed species) made available for detection over a Schottky barrier of height ξ_s, $N(\xi_s)$:

$$N(\xi_s) = \frac{\rho\upsilon}{M\dot\sigma} \int_{\xi_s}^{\infty} \tilde{f}_\xi(0, t)\, d\xi. \tag{16}$$

Equations (8), (15*b*) and (16) give rise to

$$N(\xi_s) = E_{eh}\Gamma_{\eta/\varepsilon_0} \int_{\xi_s}^{\infty} d\xi \int_{\xi}^{\infty} dx\, \frac{e^{-x/\eta}}{x^3}[1 - \cos(x/\varepsilon_0)]$$

$$= E_{eh}\Gamma_{\eta/\varepsilon_0} \int_{\xi_s}^{\infty} dx\, \frac{(x - \xi_s)e^{-x/\eta}}{x^3}[1 - \cos(x/\varepsilon_0)]$$

$$= E_{eh}\Gamma_{\eta/\varepsilon_0} \frac{e^{-\xi_s/\eta}}{\eta} \int_0^{\infty} dz\, \frac{z e^{-z}}{\left[z + \left(\frac{\xi_s}{\eta}\right)\right]^3}$$

$$\times \left\{ 1 - \cos\left[\frac{1}{\varepsilon_0}(z\eta + \xi_s)\right] \right\}, \tag{17}$$

where $E_{eh} = p_{eh}E_a$ is the fraction of adsorption energy transferred to the e–h pairs per adatom. For $\xi_s \gg \eta$ the integral

in equation (17) can be solved analytically according to

$$N(\xi_s) \cong E_{eh}\Gamma_{\eta/\varepsilon_0} \frac{\eta^2 e^{-\xi_s/\eta}}{\xi_s^3} \int_0^{\infty} dz\, e^{-z} z$$

$$\times \left[1 - \cos\left(\frac{1}{\varepsilon_0}(z\eta + \xi_s)\right) \right]$$

$$= E_{eh}\Gamma_{\eta/\varepsilon_0} \frac{\eta^2 e^{-\xi_s/\eta}}{\xi_s^3}$$

$$\times \left[1 - \frac{\left[1 - \left(\frac{\eta}{\varepsilon_0}\right)^2\right]\cos(\xi_s/\varepsilon_0) - 2\left(\frac{\eta}{\varepsilon_0}\right)\sin(\xi_s/\varepsilon_0)}{\left[1 + \left(\frac{\eta}{\varepsilon_0}\right)^2\right]^2} \right]. \tag{18}$$

From equation (18) we find that the chemicurrent yield is a decreasing function of the ratio ξ_s/η and, in addition, it depends upon ε_0. Furthermore, in the limiting case $\omega \ll \omega_0$ the single-excitation probability distribution function and the hot carrier current are independent of ε_0. As regards the approximation employed in equation (18), one observes that the approximate integral is about a factor of four larger than the exact one. Nevertheless, owing to the small value of the integral (for ξ_s/η values of interest in chemicurrent experiments it is about 6×10^{-3}) the analytical approximation can be retained.

The spectrum of the excited electrons, and consequently the chemicurrent, vanishes when the adsorption process reaches completion (equation (15*b*)). On the other hand, the chemicurrent yield (equations (16)–(18)) is independent of surface coverage provided the adsorption is active. As a matter of fact this equation can equally be applied to diatom recombination provided that E_a is substituted with $\Delta H = \frac{1}{2}D_{A_2}$, D_{A_2} being the diatom binding energy of the molecule (figure 1(a)). In the case of H adsorption on a Cu surface, experimental measurements give $N(\xi_s) \cong 10^{-2}$ electrons/atom for Schottky barriers in the range $0.55 - 0.65$ eV [4, 10]. Equation (18) is employed to evaluate the chemicurrent yield at $p_{eh} = 1$, i.e. by assuming that all exchanged energy is deposited into the e–h pairs. At this point a comment is in order about this approximation. Energy disposal via phonon excitation is expected to play a minor role in the case of light adatoms, namely in the case of a small ratio between the masses of adatom and metal atom. The classical Baule expression for energy transfer shows that this quantity scales as this mass ratio [6]. Quantum mechanically, the adatom can be elastically scattered by the lattice without any energy loss. The probability for this to occur depends on the Debye–Waller factor whose value is larger the lower the mass ratio above. In addition, in the absence of any match between the phonon band and the vibrational state of the adatom, energy disposal may occur by multiphonon excitation where, as a rule, the process with the smallest number of emitted phonons is favoured [19]. Usually the cross section for the excitation of n phonons is a factor of 10–100 larger that that for the excitation of $n + 1$ phonons [19]. Therefore, in the case of the H/Cu system the e–h excitation should prevail. As a matter of fact, this issue has been tackled in [18] where it has been found that, for this system, the phonon production has a small influence on the chemicurrent yield.

The hot electron yield, estimated through equation (18), is reported in figure 5 as full lines. As anticipated above,
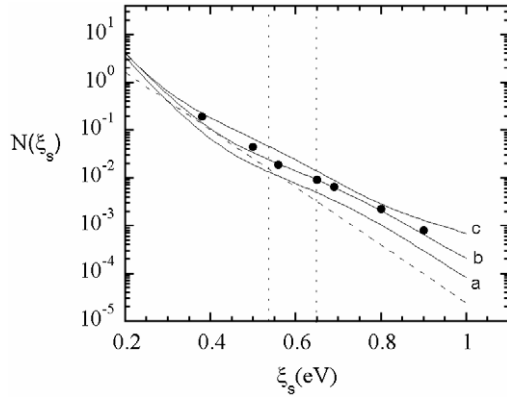
Figure 5. Number of electrons available for detection over a Schottky barrier of height ξ_s for the H/Cu system. The experimental value is about $N(\xi_s) \cong 10^{-2}$ for barriers in the energy range 0.55–0.65 eV. The curves estimated through equation (18) are shown as full lines for $E_{\mathrm{eh}} = 2.27$ eV and $\eta = 0.15$ eV, $\varepsilon_0 = 0.1$ eV (curve a); $\eta = 0.17$ eV, $\varepsilon_0 = 0.1$ eV (curve b); $\eta = 0.2$ eV, $\varepsilon_0 = 0.08$ eV (curve c). The dashed line is the chemicurrent yield computed in [14] by assuming a continuous distribution of adatom states. The full symbols are the results of the first-principles theory of [10].

the value $\varepsilon_0 \cong 0.1$ eV, used in this computation, is in accord with that obtained in [18] through *ab initio* calculations. Equation (18) yields $N(\xi_s)$ figures that are in agreement with the experimental outcome for η parameters in the range 0.15–0.2 eV, namely for mean values of energy loss in the interval 0.17–0.2 eV. Notably, these values are in good agreement with that obtained in [18]. The present results have also been compared in figure 5 to those available in the literature for the same system. Specifically, the dashed line is the $N(\xi_s)$ curve derived from master equations in the case of a continuous distribution of adatom states in the potential well. The parameters employed in the computation are [14]: $\langle \Delta E \rangle = 0.15$ eV, $\beta = 136$ eV^{-1}, $\Phi = 0.02$ s^{-1} and $K_{\mathrm{eh}}\rho_a = 2.5 \times 10^{15}$ eV s^{-1}, ρ_a and Φ being the adatom density of states and the steady state recombination rate, respectively. K_{eh} is the forward rate constant for the energy transfer between the adatom and the solid and $\beta = (kT)^{-1}$, where k is the Boltzmann constant and T the surface temperature. The full symbols in figure 5 are the chemicurrent yield obtained by the first-principles theory of [10]. It is worth noticing that the analytical result (equation (18)) is in accord with that of the *ab initio* method in a wide range of Schottky barriers and, more importantly, for similar values of the physical parameters. In fact, curve b in figure 5 has been calculated for $\langle \Delta E \rangle = 0.18$ eV that agrees well with the value $\langle \Delta E \rangle = 0.16$ eV estimated in [18].

In [15] the chemicurrent yield has been computed by exploiting the analogies with spectroscopic processes leading to the x-ray edge singularity. In that model the probability of the single pair excitation is a function of the switching rate of the perturbation and exhibits an exponential behaviour similar to that obtained here in terms of η [20]. In fact, these two quantities have the same order of magnitude, both being in the range 0.1–0.5 eV.

The phenomenological model discussed so far can be used to interpret the isotope effect on chemicurrents. Recently, this issue has been considered in detail in [21] on the grounds of experimental data on hot carrier generation in H and D adsorption on a Ag/Si diode. The H/D-chemicurrent efficiency ratio is found to be $R_1 \cong 4$ and $R_2 \cong 7$ for Schottky barrier heights of 0.46 eV and 0.7 eV, respectively [21]. By noting that the vibrational states in the anharmonic D-Ag potential well are closer to each other than for the H-Ag system by a factor of $\sqrt{2}$, one can assume that $\frac{\eta_{\mathrm{H}}}{\eta_{\mathrm{D}}} \approx \sqrt{2}$. This is in accord with the physical meaning of η, as it stems from Gunnarsson and Schönhammer's approach, where η^{-1} is shown to be proportional to the crossing time of the adsorbate level, namely to the inverse of the atom velocity, υ_a. Since $\upsilon_a \cong (D_{A_2}/m_A)^{1/2}$ the crossing time is proportional to the square root of the adatom mass. Consequently, $\eta_{\mathrm{H}}/\eta_{\mathrm{D}} \approx (m_{\mathrm{D}}/m_{\mathrm{H}})^{1/2}$ as reported above. A similar argument has been employed in [15] in discussing the scaling of the 'switching-on rate' of the perturbation with the depth of the adsorption potential well. By assuming the ratio η/ε_0 to be the same for both species, the efficiency ratio given through equation (18) reads

$$R_i \approx \frac{\eta_{\mathrm{H}}^2}{\eta_{\mathrm{D}}^2} \exp\left[-\xi_{s,i}\left(\frac{1}{\eta_{\mathrm{H}}} - \frac{1}{\eta_{\mathrm{D}}} \right) \right] = 2\exp\left[\frac{\xi_{s,i}}{\eta_{\mathrm{H}}}(\sqrt{2}-1) \right]. \tag{19}$$

Equation (19) is consistent with both the experimental values R_1 and R_2 above, for $\eta_{\mathrm{H}} \cong 0.24$ eV that is $\langle \Delta E \rangle \cong 0.21$ eV (figure 3(b)).

Before concluding a comment is in order in connection with both the estimate of the average over the P_1 distribution (equation (14)) and the results of [14]. As regards P_1, it is worth recalling that this distribution, that is linked to single e–h excitations, is assumed to hold for each round trip of the atom trapped in the potential well. Accordingly, the rate of e–h pair generation, with energy in the range $w - w + \mathrm{d}w$, is equal to $n(w)\phi P_1(w)\,\mathrm{d}w$ where ϕ is the adsorption rate and $n(w)$ the number of scattering events before thermalization. The present computation therefore rests on the assumption $n(w) \approx E_a/w$. As far as the results of [14] are concerned, one observes that this statistical model is restricted to the reactive adsorption under steady state conditions. It deals with a mobile adlayer and a continuous set of adatom states in the adsorption well where, for each of them, an occupation number by adatoms can be defined. The steady state populations are dictated by recombination and energy disposal processes, namely the flux of adatoms entering a given level, owing to the energy disposal, equals the sum of the fluxes leaving the level because of both recombination and energy dissipation phenomena. Although based on some approximations, the theory developed in [14] has the merit of highlighting the interplay between the *electron* and the *adatom* energy distribution functions at steady state. To be specific, by denoting with $\tilde{f}_a(E)$ the non-equilibrium component of the energy distribution function of the adatoms, one obtains [14]

$$\tilde{f}_z = Q\left[\int_z^{X^*} \tilde{f}_a(X')\,\mathrm{d}X' \int_z^{X'} \Gamma(\zeta)\,\mathrm{d}\zeta - \int_0^{X^*-z} \tilde{f}_a(X')\,\mathrm{d}X' \right.$$
$$\left. \times \int_z^{X^*-X} \mathrm{e}^{-\zeta}\Gamma(\zeta)\,\mathrm{d}\zeta \right], \tag{20}$$

where $z = \beta\xi$, $X = \beta E$ and $X^* = \beta E^*$, E^* being the energy of the upper bound level in the adsorption well. In equation (20) $\Gamma(\zeta)$ is the state to state transition probability for the energy transfer $\Delta E = \zeta/\beta$ via e–h excitation. The Q term in equation (20) depends on both β and z. Furthermore it was demonstrated in [3] that, in the case of a discrete set of vibrational levels, the energy distribution of the adatoms can be approximated as $f_a(E_n) \cong e^{-\beta E_n} + \Phi/\sigma K$, where K is the rate constant for energy disposal, σ the surface coverage and Φ the recombination rate at steady state. Therefore, at higher energies the distribution becomes uniform and equal to $f_a(E_n) \cong \Phi/\sigma K$. This implies that the non-equilibrium function $\tilde{f}_a(E)$, in equation (20), is different from zero for $E > E_0$ where $\beta E_0 = X_0 = -\ln(\Phi/\sigma K)$ and is approximately independent of temperature [3]. As a consequence the integral in equation (20) depends on temperature through the z variable. In equation (20) a temperature-dependent term also arises from the detailed balance that is achieved by taking into account the adatom excitation in the potential well caused by the relaxation of the electron gas. Therefore, the chemicurrent yield estimated by using equation (20) is expected to be temperature dependent since the integration over the electron spectrum has to be performed in the ξ variable [14]. On the other hand, in the model presented here $N(\xi_s)$ is nearly independent of temperature. This is due to fact that the process of adatom excitation by hot carriers has not been included in equation (2).

In summary, the temporal and spatial dependence of the spectrum of hot electrons in exothermic adsorption on metal surfaces has been analysed by means of the Boltzmann transport equation. This energy distribution function allows one to compute the number of electrons made available for detection over a Schottky barrier, i.e. to model the chemicurrent yield. This current is found to depend on the average value of the energy deposited in the e–h pair, on the Schottky barrier and on adsorption energy. The results derived from the theory compare favourably with the experimental chemicurrents of the H/Cu system, as well as with results of first-principles theory for a mean value of the energy loss that is in accord with *ab initio* calculation.

References

[1] Harris J and Kasemo B 1981 *Surf. Sci.* **105** L281
[2] Jackson B, Sha X and Guvenc Z B 2002 *J. Chem. Phys.* **116** 2599
[3] Molinari E and Tomellini M 2006 *Catal. Today* **116/1** 30
[4] Nienhaus H, Bergh H S, Gergen B, Majumdar A, Weinberg W H and McFarland E W 1999 *Phys. Rev. Lett.* **82** 446
[5] Gergen B, Nienhaus H, Weinberg W H and McFarland E W 2001 *Science* **294** 2521
[6] Nienhaus H 2002 *Surf. Sci. Rep.* **45** 1
[7] Shenvi N, Roy S, Parandekar P and Tully J 2006 *J. Chem. Phys.* **152** 154703
[8] Schönhammer K and Gunnarsson O 1980 *Phys. Rev.* B **22** 1629
[9] Falcone G and Sroubek Z 1988 *Phys. Rev.* B **38** 4989
[10] Trail J R, Brham M C, Bird D M, Persson M and Holloway S 2002 *Phys. Rev. Lett.* **88** 166802
[11] Lindenblatt M, Pehlke E, Duvenbeck A, Rethfeld B and Wucher A 2006 *Nucl. Instrum. Methods Phys. Res.* B **246** 333
[12] Lindenblatt M, van Heys J and Pehlke E 2006 *Surf. Sci.* **600** 3624
[13] Mizielinski M S, Bird D M, Persson M and Holloway S 2007 *J. Chem. Phys.* **126** 034705
[14] Tomellini M 2007 *Surf. Sci.* **601** 2260
[15] Gadzuk J W 2002 *Phys. Chem.* B **106** 8265
[16] Ashcroft N W and Mermin N D 1988 *Solid State Physics* (Hong Kong: Holt, Rinehart and Winston)
[17] Šunjić M and Lucas A A 1971 *Phys. Rev.* B **3** 719
[18] Trail J R, Bird D M, Persson M and Holloway S 2003 *J. Chem. Phys.* **119** 439
[19] Persson B N J and Avouris Ph 1997 *Surf. Sci.* **390** 45
[20] Gadzuk J W and Metiu H 1980 *Phys. Rev.* B **22** 2603
[21] Krix D, Nünthel R and Nienhaus H 2007 *Phys. Rev.* B **75** 073410